JOURNAL OF GUIDANCE, CONTROL, AND DYNAMICS
Vol. 18, No. 2, March–April 1995

Onboard Star Identification Without A Priori Attitude Information

Eleanor A. Ketchum*
NASA Goddard Space Flight Center, Greenbelt, Maryland 20771
and
Robert H. Tolson†
George Washington University, Hampton, Virginia 23681-0001

Many algorithms used today determine spacecraft attitude by identifying stars in the field of view of a star tracker. However, each of these methods require some a priori knowledge of the spacecraft attitude. Some algorithms have been extended to implement a computation-intense full-sky scan. Others require large data bases. Both storage and speed are concerns for autonomous onboard systems.This paper presents an algorithm that, by discretizing the sky and filtering by visual magnitude of the brightest observed star, provides a star identification process that is computationally efficient, compared to existing techniques. A savings in onboard storage of over 80% compared with a popular existing technique is documented. Results of random tests with simulated star fields are presented without false identification and with dramatic increase in speed over full-sky scan methods.

Introduction

LOW Earth orbit satellites have traditionally used the stars for fine tuning the spacecraft attitude. Gimbaled and fixed head image dissector star cameras have given way recently to the more accurate charge-coupled device (CCD) star tracker. These trackers can determine the visual magnitude and angular position of a number of stars in the field of view (FOV). With an a priori attitude estimate, well-documented methods[1–7] can identify observed stars and hence the spacecraft attitude. Most of these methods are variations of the method of matching the angular separation of observed star pairs.[1] Recently, neural network technology has been applied to the star pattern recognition problem[8]; although the work looks promising for the future, the method requires a star tracker FOV more than six times larger than what will be considered for this study.

Without an a priori attitude estimate, the task becomes more difficult. In practice, a spacecraft sun sensor and magnetometer are often used to determine a coarse a priori attitude estimate. However, circumstances may arise that make this impossible. For instance, the spacecraft may not have operating secondary sensors due to mission budget restrictions or hardware failure, or the sensors may be occulted. Also, many missions have minimal ground contact, making a priori attitude estimates difficult to uplink.

Instruments could be damaged or destroyed if exposed to direct sunlight, and without attitude knowledge, a spacecraft could exit Earth shadow in a vulnerable orientation. Furthermore, initial acquisition without coarse sensors, as in the case with the Solar and Heliospheric Observatory, the X-Ray Timing Experiment, and some of the small explorers, becomes difficult, especially in the case of contingency.

There have been a few methods that examine this lack of a priori attitude information problem.[9,10] Some have expanded their normal methods to include a full-sky scan[9]; this process is in general computation intensive. On the other hand, Van Bezooijen[10] has successfully taken a variation of the method of matching angular separations of star pairs, which can determine attitude several orders of magnitude faster than a full-sky scan. This process is, however, computer storage intensive since it requires storing the list of all possible observed star pair angular separations in order of size.

This paper presents an algorithm for identifying observed stars onboard spacecraft without an a priori attitude estimate while improving storage and speed over previous methods. The algorithm needs less storage than the Van Bezooijen method and less time than a full-sky scan. The algorithm takes primary advantage of the rarely used visual magnitude, particularly of the brightest observed star. A subset of points evenly spaced on the sphere, which represent the centers of subcatalogs created to compare against observed stars, forms a discrete list of regions that the tracker can be viewing. Given the magnitude of the brightest observed star, it is possible to determine the regions of the sky where the tracker cannot be pointing. For the remaining regions, a subcatalog of stars is created, and using the traditional angular separation method, the observed stars are identified. Although the algorithm presented here compares angular separations with observed stars until a match is found, any method that assumes some a priori attitude information can be used for this final step.

Results from analysis show that, for the worst case, only 48% of the sky needs to be checked. However, even in the worst case, it is unlikely that all possible regions need to be checked before a match is found since the regions are searched in order of likelihood that each would contain a match.

Details of the algorithm and some analytical results, including how many checks are required for a given observed magnitude and the relative speed at which a single check can be performed, are presented below. It will be shown that storage requirements are improved from previous methods without impacting the operational feasibility of the method.

Hardware and Star Catalog Assumptions

Although the general algorithm is flexible enough to be used for any star tracker (e.g., FOV size), specifications for the Ball CT-601 Solid State Star Tracker,[11] which is scheduled to be used on several upcoming missions, were used for this study. Also, other CCD star trackers to be flown in the near future have similar specifications. The tracker has an $8 \times 8\text{-deg}^2$ FOV; however, a 4-deg-radius circular FOV was assumed since star observations in the corners of FOVs are often not considered. The Ball tracker provides the position in

Received Aug. 27, 1993; revision received June 16, 1994; accepted for publication Sept. 8, 1994.

*Flight Dynamics Engineer, Flight Dynamics Division; currently a Ph.D. candidate in Astronautics at the George Washington University Joint Institute for the Advancement of Flight Sciences.

†Professor, Joint Institute for the Advancement of Flight Sciences, Mail Stop 269, NASA Langley Research Center. Associate Fellow AIAA.

the FOV with a ±3-arcsec bias error and a ±5-arcsec total random error. It can provide a magnitude measurement to within ±0.2.

Although the magnitude measurement specifications for the Ball Aerospace Star Tracker[11] are stated as ±0.2 magnitude, and consequently assumed to be instrument magnitude, it is also assumed that the appropriate transfer function can be used to convert to visual magnitude M_v. The CCD tracker is more sensitive to red stars; a red star may have a faint M_v while appearing bright in the CCD FOV. An improved star catalog that uses more accurate red star observations is, at the time of this report, in production at the Goddard Space Flight Center (GSFC) Flight Dynamics Facility. A particular CCD tracker can also be calibrated in flight by viewing reference stars of representative spectral classes.

The tracker is capable of tracking up to five stars at a time and can search the entire FOV for the five brightest. This study assumes an inertially fixed spacecraft; in the case of a tumble, it is assumed that any rate can be stopped before the star identification process begins. Once stationary, the tracker can acquire a full field in 5 s.

For the purposes of this study, the standard GSFC Flight Dynamics Division (FDD) Multi-Mission System star catalog was used.[12] This catalogue has been used for many missions, including the Gamma Ray Observatory and the Upper Atmospheric Research Satellite. The catalog contains 8949 stars ranging in visual magnitude from -1.65 to 6.5 M_v.

Algorithm

Onboard Data Base

The task of this algorithm is to determine where the stationary star tracker is looking based only on the data from the tracker. In addition, the direction is to be identified with minimal stored data and in a short time.

As with any star identification algorithm, the onboard data base must contain the right ascension (RA), declination (DEC), and magnitude (MAG) of the reference catalog stars. In addition to the reference catalog, the algorithm requires other information onboard, described below.

The development of this minimal onboard storage method begins by dividing the celestial sky into a nearly evenly spaced, minimally overlapping, complete covering of the sphere. Ideally, the vertices of a regular polyhedron represent evenly spaced points on a sphere. Unfortunately there is a limited number of regular polyhedrons, none of which provide enough points. However, the faces of the polyhedron can be divided into equal polygons with the vertices projected on the sphere. Clearly, the least distortion will result from the polyhedron with the most, and consequently smallest, faces. Also, the triangular or square faces would be the simplest to subdivide. The isocohedron, a regular 20-sided polygon whose faces are equilateral triangles, fits both requirements. For the 4-deg-radius FOV case considered, each face is then divided into 121 smaller triangles, 11 across a side; however, this isocohedron technique of dividing up the celestial sphere is important not only in its minimal covering, but also in its robustness, unlike strictly regular polyhedrons, to FOV size. When projected on the sphere, the vertices of these smaller triangles become the 1212 centers of 4-deg-radius FOVs that completely cover the sphere, called subcatalog centers. Each star in the catalog appears in from one to three subcatalogs, due to some overlap in the covering.

Each of these subcatalog centers has a visual magnitude associated with it corresponding to the magnitude of the brightest catalog star within a 4-deg-radius, called a primary bright star (Fig. 1). The right ascension and declination of each subcatalog center and the magnitude of the associated primary bright star is stored from brightest to dimmest in the onboard data base. Note that the actual subcatalogs are not stored, but are formed onboard from the database.

There is a nonzero probability that no primary bright star appears in an observed FOV. The observed brightest star is then called a secondary bright star (Fig. 2). These stars have been identified in the reference catalog by solving a constrained equation. A star is a secondary bright star if and only if a 4-deg-radius FOV can be positioned to contain the secondary bright star but no brighter star (Fig. 3). Mathematically, a solution is sought for the problem:

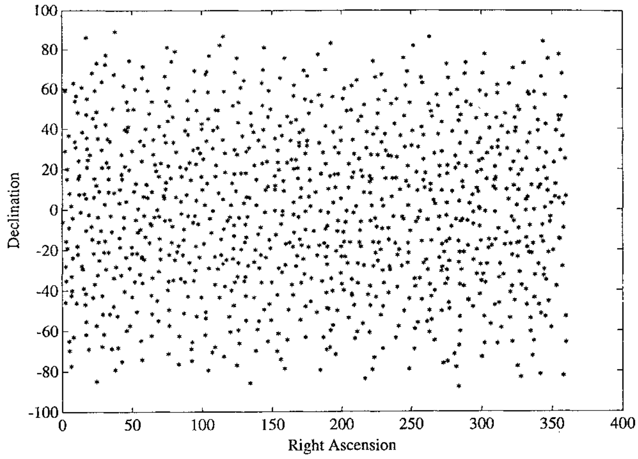

Fig. 1 Primary bright stars.

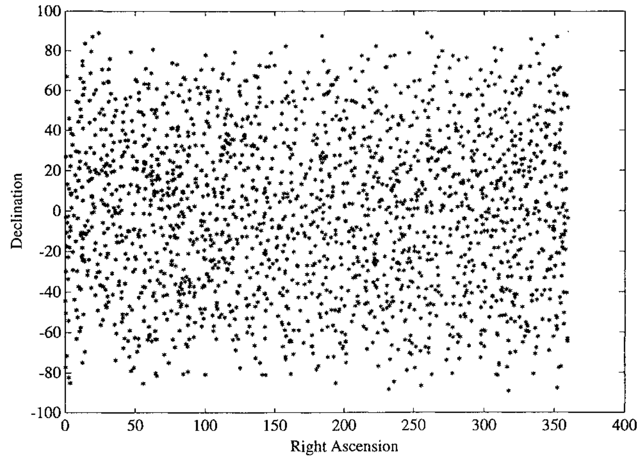

Fig. 2 Secondary bright stars.

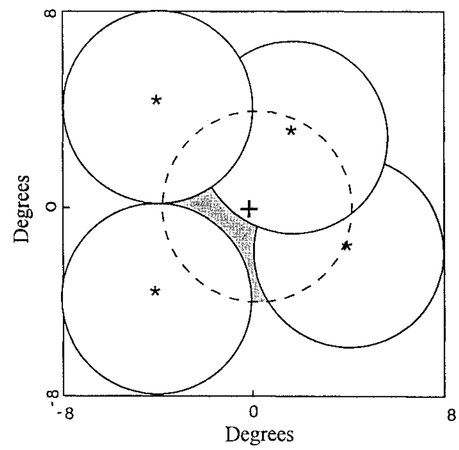

Fig. 3 Identify secondary bright stars.

Solve

$$x^2 + y^2 = 16 \tag{1}$$

Subject to

$$(x - x_i)^2 + (y - y_i)^2 > 16 \tag{2}$$

where x_i, y_i are the coordinates of the planar projection of all the brighter neighbor stars within 8 deg of the secondary bright-star candidate.

If the solution exists, then x and y correspond to the center of a FOV that contains the secondary bright star and no brighter neighbor.

Table 1 Onboard data base

Item	Dimension/description	Total words
Catalog	8949 stars by 3 (RA, DEC, MAG)	26,847
Subcatalog centers	1212 by 3 (RA, DEC, MAG)	3,636
Secondary bright stars	2001 by 2 (MAG and weight)	4,002
	1267 by 1	1,267
	643 by 2	1,286
	91 by 3	273
	(indices of up to 3 subcatalog centers containing the star)	
Total		37,311

Table 2 Total onboard storage

Item	Total bytes
Onboard data base	74,586
Code	32,000
Algorithm overhead	7,052
Total	113,638

There are 2001 secondary bright stars associated with the reference catalog used for this study.[12]

These secondary bright stars can have a degree of likelihood, or weight, associated with them based on the preceding equations. If a solution does exist to the above equations, there is in general a two-dimensional continuum of solutions. The area of this continuum is a measure of the likelihood of that star being observed as the brightest star in the FOV. For instance, the continuum of solutions for a star with no brighter star within an 8 deg radius corresponds to the area of the entire 4-deg-radius circle and is therefore among the most likely candidates. The area associated with each secondary bright star was determined by creating a grid of points 0.5 deg apart on the sphere and then simply counting the points that satisfy Eq. (1) and the constraints in Eq. (2). A typical 4-deg FOV would contain about 90 such points.

Finally, the onboard data base contains, for each of the 2001 secondary bright stars, the magnitude and weight of the star as well as the indices of the one, two, or three associated subcatalog centers. This resulted in 1267 secondary bright stars being associated with just one subcatalog center, 643 with two, and 91 with three.

Table 1 summarizes the contents of the onboard data base.

Total Required Onboard Memory

The algorithm itself, described below, requires approximately 500 lines of code, or less than 32,000 bytes. As will be explained in detail below, the algorithm needs to have, at any one time, a maximum of 600 subcatalog center indices associated with primary bright stars, 2826 indices of subcatalog centers associated with secondary bright stars, and 100 words of other overhead including observed and candidate star pairs.

Table 2 summarizes the total required onboard memory, assuming 2-byte integers.

The Van Bezooijen method[10] requires 840,000 bytes plus 24,750 bytes for the 4125 guide star reference catalog, for a total of 864,750 bytes. Also, the FOV that Van Bezooijen considers is 11.5 × 11.5 deg, and he states that there is an onboard storage increase as the FOV size decreases. Therefore, the algorithm considered in this study represents greater than 87% decrease in onboard storage from the Van Bezooijen method. Further, the total onboard data base requirement is only 39% greater than storing the star catalog alone, a component necessary for autonomous attitude determination regardless of which algorithm is used to identify the stars.

Algorithm

The process is shown in Fig. 4 and begins with input of the measure of the magnitude of the up to five brightest stars in the FOV, along with the position of each star in ±4 deg horizontal and vertical (H and V, respectively). The algorithm identifies the visual magnitude of the brightest star in the observed FOV and calculates the angular separations of the brightest star with up to four other observed stars (see "Pre-process observed stars" in Fig. 4). Each subcatalog center that has a primary bright star with visual magnitude within ±0.2 M_v is identified (see first box in "Check primary bright stars" in Fig. 4). To minimize search time, the subcatalog center processing order is based on the difference between the observed magnitude of the brightest star. It is important to note that any a priori attitude knowledge, e.g., knowledge of location in orbit, may eliminate some subcatalog center choices. To process a subcatalog center, an actual subcatalog of stars is extracted from the reference catalog. The subcatalog contains all stars within an 8 deg radius of the subcatalog center (see second box in "Pre-process reference subcatalogs" in Fig. 4). There may be more than one star in the appropriate magnitude range in the subcatalog, so for each such star the angular separation between the star and its neighbors are calculated and compared to those for the observed stars (see "Angular comparison check" in Fig. 4).

Although mission specific, a match is found when a "triplet" is discovered. A triplet occurs when the angular separations between the bright star being checked and two of its neighbors, the magnitude of each neighbor (see third box in "Angular comparison check" in Fig. 4), and the angular separation between the neighbors (see final box in "Angular comparison check" in Fig. 4) match the subcatalog within the specified accuracy. This triplet method is well documented[1] and has been used extensively in the past.

If the entire list of identified subcatalog centers is checked without a "triplet" match, a list of subcatalog centers is generated that 1) contains subcatalog centers that have a secondary brightest star in the appropriate magnitude range and have not been checked above and 2) is ordered by descending weight (see "Check secondary bright stars" in Fig. 4). Each of these is checked using the same process as was used for the primary bright-star subcatalog center list.

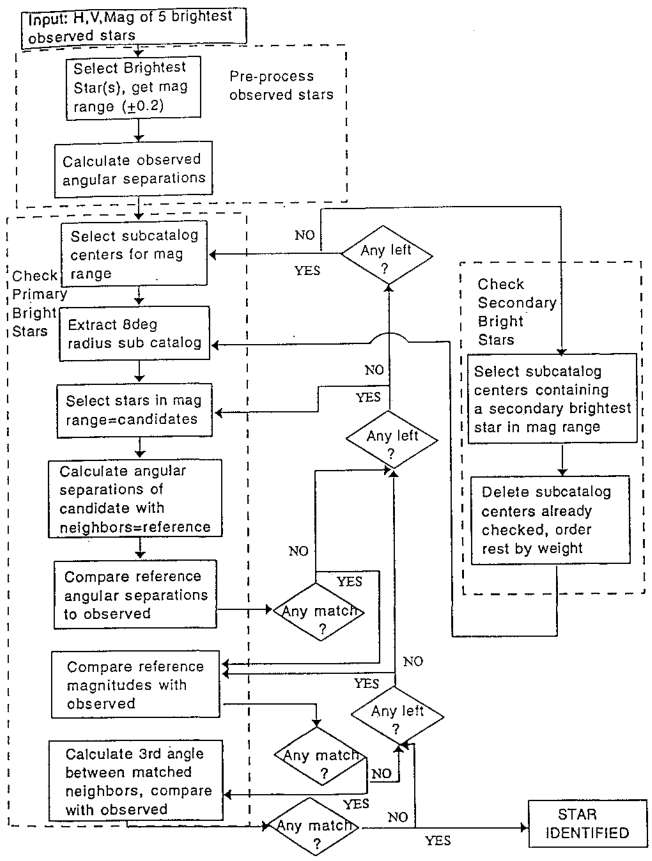

Fig. 4 Flow diagram.

This completes the description of the algorithm. Like any algorithm, there is a nonzero probability that no star will be found. There are several reasons why this could happen and therefore several precautions and corrective actions to take.

A nonidentification could mean that, due to underestimating the M_v error, the magnitude range and consequently the list of subcatalog centers was too small to include the correct one. Clearly, in lieu of accurate knowledge of the M_v error, a conservative estimate is essential. Therefore, if a star is not identified, the process should be repeated with a larger M_v range. Note also that the magnitude measurements can, and should be, calibrated throughout the mission, thus reducing the M_v error.

A nonidentification could also mean that the observed brightest star is not in the catalog. If the brightest star is a variable star, as very bright stars often are, it will not be identified, since variable stars are flagged (and consequently do not appear) in the reference catalog considered for this study. Similarly, if the brightest observed star is not a star at all, it will not appear in the reference catalog. The identification process should then be repeated considering the second brightest observed star, along with the three remaining neighbors.

A nonidentification could occur if the brightest reference star in the FOV is for some reason not reported by the tracker. Without any intervention, due to some overlap in subcatalog centers, there is a likelihood that the brightest star that is reported is a primary bright star for a neighboring subcatalog center or is itself a secondary bright star. Unfortunately, if there is still no identification, the only corrective action would be to change the observed FOV, if only by a small attitude maneuver to the spacecraft.

Finally, the uniqueness of observed triplets is a function of accuracy, a mission-specific concern, and is not addressed in this study.

Premission Analysis

When using a star tracker with a different FOV size, it will be necessary to create the appropriate set of minimum overlapping, evenly spaced, covering set of subcatalog centers. The isocohedron technique described above can still be used, remembering that the vertices of the small triangles represent the center of a FOV and to make sure that there are no gaps in the covering on the sphere. For reference, Table 3 shows the number of points (subcatalog centers) on the sphere and FOV size. Simple geometry relates the number of points on the sphere (N) as a function of the number of smaller triangles across a side (n), described in Eq. (3), where the number of smaller triangles on each face is n^2:

$$N = (n-1)E + V + \left(\tfrac{1}{2}\right)(n-2)(n-1)F \tag{3}$$

where $E = 30$ edges, $V = 12$ vertices, and $F = 20$ faces. These points are centers of FOVs (4-deg radius for this study) that identify the primary bright stars and then become subcatalog centers. The subcatalogs created onboard in real time should be at least 2 times the radius of the actual FOV to ensure identification even if the true (observed) FOV center is actually several degrees from the subcatalog center.

Table 3 Number of subcatalog centers and FOV size

Radius of FOV	Number of triangles along edge	Total number of subcatalog centers
≥19.427	2	42
≥12.459	3	92
≥10.572	4	162
≥ 8.558	5	252
≥ 6.968	6	362
≥ 6.180	7	492
≥ 5.422	8	642
≥ 4.762	9	812
≥ 4.351	10	1002
≥ 3.960	11	1212
≥ 3.604	12	1442
≥ 3.355	13	1692
≥ 3.117	14	1962
≥ 2.895	15	2252
≥ 2.729	16	2562

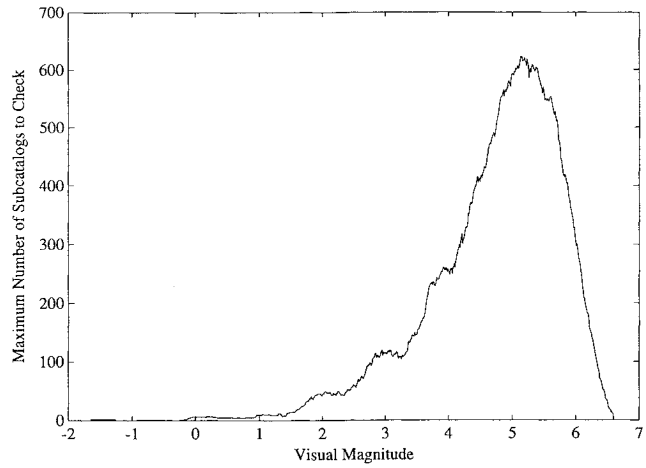

Fig. 5 Visual magnitude of observed stars vs maximum number of subcatalogs to check.

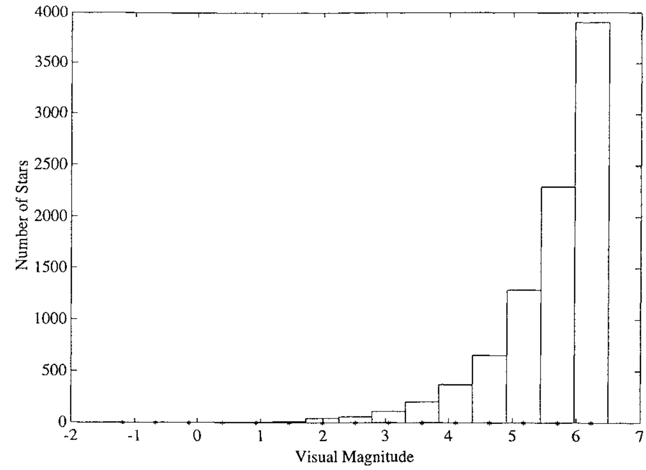

Fig. 6 Histogram of stars by visual magnitude.

Computation Costs

The computational time to identify a star depends on the number of subcatalog centers that are searched. Figure 5 shows the total number of subcatalogs (of the 1212 total) that would need to be checked based on the visual magnitude brightest star in the observed FOV. This includes also the possibility that the observed brightest star is actually a secondary bright star. The most subcatalogs that ever need to be checked is 623 (about half of the sky) when the magnitude is 5.2. The mean is 154, or about one-eighth of the sky.

The stars are not evenly distributed by magnitude, and Fig. 6 shows a histogram of the number of stars in the entire star catalog by visual magnitude. About half (about 4300 of 8949) of the stars fall between 4.5 and 5.9. Of these, according to Fig. 5, between 375 and 623 subcatalogs would need to be checked. For the other half of the stars, less than 375 subcatalogs (just over one-fourth of the sky) need to be checked. The reason that the abundant dim stars require so few total checks lies in the concept of the secondary bright stars described in Eqs. (1) and (2). If the brightest observed star is very dim, there are only a few places in the sky that the tracker could be viewing.

Therefore, at worst, half the sky would need to be checked. Bear in mind, however, that it is unlikely the entire list of 623 subcatalogs will need to be checked in that the weight, as described above, of the subcatalog centers at the bottom of the list of subcatalog centers is very low. In fact, over half of the secondary stars have weight below 5 of 90, not likely to be the observed brightest star. A histogram showing the number of secondary bright stars (2001 total) with various weights is given in Fig. 7.

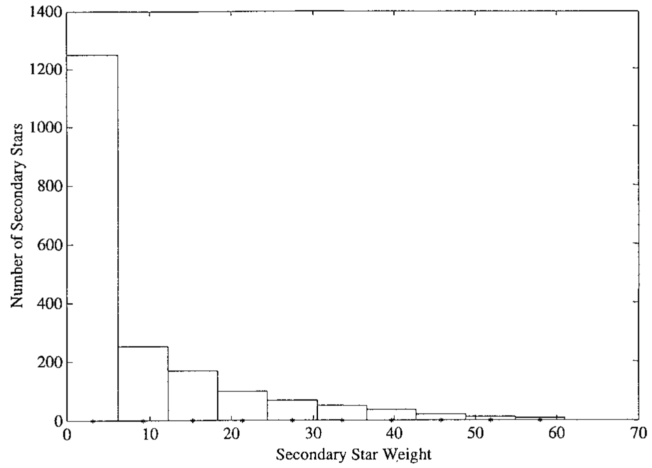

Fig. 7 Histogram of secondary bright stars by weight.

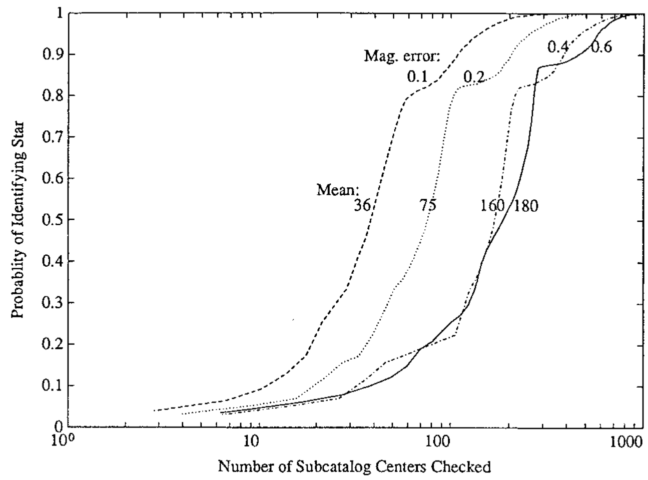

Fig. 8 Probability curves.

Preliminary Test Results

Random Tests

Test data have been created by randomly choosing a direction, selecting up to five brightest stars within the FOV, adding a random error to both the position (± 10 arcsec uniform) and magnitude (± 0.2 M_v uniform), and converting the positions to H and V degrees.

A single check of a subcatalog takes roughly 0.125 s (wall clock time) on a 486 50-MHz personal computer. Again, refer to Figs. 5–7 to get an overall idea of the maximum numbers of checks necessary given the magnitude of the observed brightest stars. The maximum time is therefore about 78 s, or 1.3 min.

Of the 50 test runs randomly placed around the sphere, the longest actual time to find the star was approximately 60.1 s, and the average was 9.53 s. Of the 50 brightest stars identified, 75% turned out to be primary bright stars and 25% secondary bright stars. Each of these random tests resulted in a correct identification.

Effect of Magnitude Error

Until this point, the M_v error has been assumed to be strictly ± 0.2. It is of interest, however, to determine the influence of larger and smaller M_v errors on the length of time to identify the observed stars. To do this study, 16,812 points on the sphere were created by dividing the isocohedron faces, described above, into 1681 smaller triangles, 41 across a side. The brightest reference catalog star within 4 deg of each point was determined. Then the list of subcatalog centers associated with primary bright stars of the appropriate magnitudes corresponding to each of ± 0.1, ± 0.2, ± 0.4, and ± 0.6 errors in M_v was created. The test counts the number of subcatalogs necessary to check to find the first one in the list (checked from smallest to largest magnitude) within 4 deg of the observed brightest star.

If no subcatalog is found within 4 deg of the observed brightest star, then a weighted list, as described above, of subcatalog centers associated with the appropriate secondary bright star (for each of the M_v error ranges) is created. The counting continues until the first subcatalog center less than 4 deg from the observed brightest star is discovered.

Therefore, for each of the 16,812 points on the sphere, the number of subcatalogs necessary to check based on the magnitude of the observed brightest star as seen from that point is determined. Figure 8 shows the probability curves for each of the M_v errors.

From Fig. 8, it can be seen that if the M_v error is halved from the specified value (0.2 M_v), the mean (and maximum) is also halved. Similarly, if the M_v is doubled, so is the mean (the maximum is not quite doubled); yet is still acceptable (i.e., a savings over searching the whole sky, or all of the 1212 subcatalogs). The linear relationship does not hold as the error is increased to ± 0.6; the results show better than three times the ± 0.2 mean, again still acceptable.

The analytical tests show that a linear improvement results from calibrating the star tracker to better than the specified ± 0.2 M_v measurement uncertainty. Conversely, a higher M_v error linearly affects the results up to a point and then tapers off, so that an error up to ± 0.6 still results in a savings over a full-sky scan.

Conclusions

This paper presented an algorithm that identifies the brightest star and two neighbors in an observed FOV using only the observed star data and without the benefit of a priori attitude information. Unlike traditional methods, visual magnitude is used to determine regions of the sky that the star tracker could not be viewing. The onboard storage requirement is low compared to current methods, whereas the algorithm should be faster than a full-sky scan. The algorithm can be adjusted for mission requirements and instrument size and accuracy.

Acknowledgment

This research was funded in part by NASA Langley Research Center cooperative agreement NCC1-104. This research is in partial fulfillment of a Doctoral degree for the first author. Preliminary results were presented at the AAS International Symposium for Space Flight Dynamics, MD, May 1993.

References

[1]Gottlieb, D. M., "Star Identification Techniques," *Spacecraft Attitude Determination and Control*, edited by J. R. Wertz; Kluwer, Dordrecht, The Netherlands, 1978, pp. 259–266.

[2]Kosik, J. C., "Star Pattern Identification Aboard an Inertially Stabilized Spacecraft," *Journal of Guidance, Control, and Dynamics*, Vol. 14, 1991, pp. 230–235.

[3]Gambardella, P., "Algorithms for Autonomous Star Identification," NASA TM-84789, Oct. 1980.

[4]Junkins, J. L., White, C. C., and Turner, J. D., "Star Pattern Recognition for Real Time Attitude Determination," *Journal of Astronautical Sciences*, Vol. 25, No. 3, 1977, pp. 251–270.

[5]Junkins, J. L., and Strikwerda, T. E., "Autonomous Attitude Estimation via Star Sensing and Pattern Recognition," *Proceedings of the Flight Mechanics and Estimation Theory Symposium*, NASA Goddard Space Flight Center, Greenbelt, MD, Oct. 1978, pp. 127–147.

[6]Strikwerda, T. E., Junkins, J. L., and Turner, J. D., "Real-Time Spacecraft Attitude Determination by Star Pattern Recognition: Further Results," AIAA Paper 79-0254, Jan. 1979.

[7]Sheela, B. V., Shekhar, C., Padmanabhan, P., and Chandrasekhar, M. G., "New Star Identification Technique for Attitude Control," *Journal of Guidance, Control, and Dynamics*, Vol. 14, No. 2, 1991, pp. 477–480.

[8]Williams, K. E., Strikwerda, T. E., Fisher, H. L., Strohbehn, K., and Edwards, T. G., "Design Study: Parallel Architectures for Autonomous Star Pattern Identification and Tracking," AAS Paper 93-102, Feb. 1993.

[9]Strikwerda, T. E., and Fisher, H. L., "A CCD Star Camera Used for Satellite Attitude Determination,"*Proceedings of the 1988 Summer Computer Simulation Conference* (Seattle, WA), 1988.

[10]Van Bezooijen, R. W. H., "Autonomous Star Referenced Attitude Determination," *Journal of Guidance, Control, and Dynamics*, Vol. 68, 1989, pp. 31–52; also American Astronomical Society, Paper 89-003.

[11]Specifications sheet for the CT-601 Solid State Star Tracker, Ball Aerospace Systems Group, Electro-Optics/Cryogenics Division, Boulder, CO.

[12]McLaughlin, S., and Slater, M., *SKYMAP Star Catalog Data Base Generation and Utilization*, NASA Goddard Space Flight Center, Flight Dynamics Division Publication FDD/554/001, Feb. 1990; also Multi-Mission System Run Catalog Version 4, Jan. 1992.